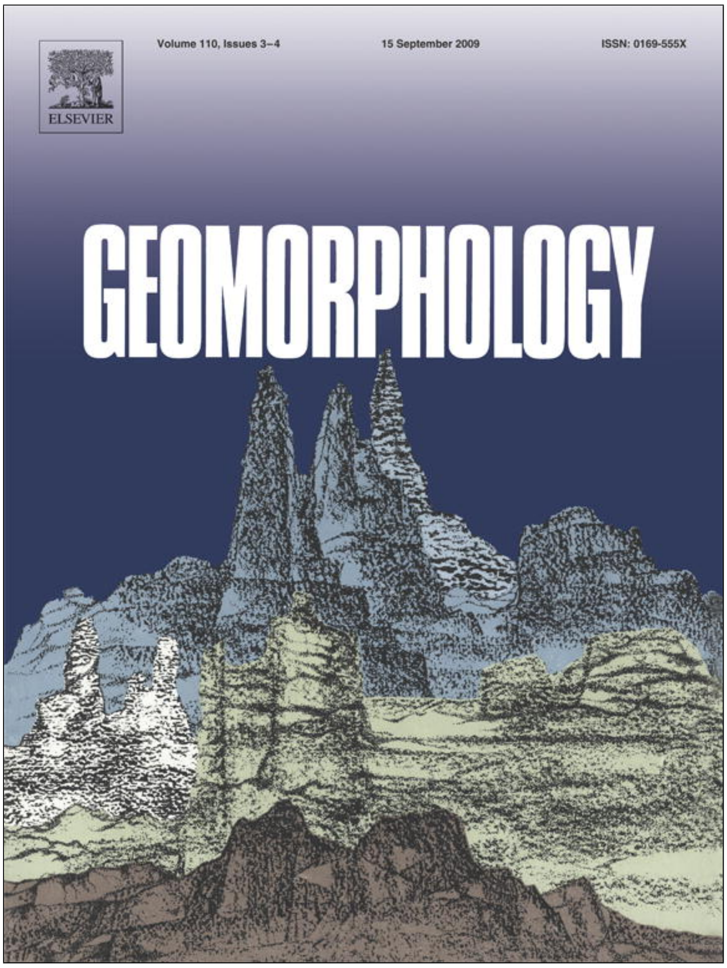
Volume 110, Issues 3–4
15 September 2009
ISSN: 0169-555X
ELSEVIER
GEOMORPHOLOGY

Geomorphology 110 (2009) 152–161

Contents lists available at ScienceDirect

Geomorphology

journal homepage: www.elsevier.com/locate/geomorph

Quantification of spatial gradation of slope positions

Cheng-Zhi Qin [a], A-Xing Zhu [a,b,*], Xun Shi [c], Bao-Lin Li [a], Tao Pei [a], Cheng-Hu Zhou [a]

[a] State Key Laboratory of Resources and Environmental Information System, Institute of Geographic Sciences and Natural Resources Research, CAS, Beijing 100101, China
[b] Department of Geography, University of Wisconsin-Madison, 550N, Park Street, Madison, WI 53706-1491, USA
[c] Geography Department, Dartmouth College, 6017 Fairchild, Hanover, NH 03755, USA

ARTICLE INFO

Article history:
Received 16 October 2008
Received in revised form 2 April 2009
Accepted 3 April 2009
Available online 14 April 2009

Keywords:
Slope position
Spatial gradation
Prototype
Similarity
Fuzzy membership
Grid DEM

ABSTRACT

Transition between slope positions (e.g., ridge, shoulder slope, back slope, foot slope, and valley) is often gradual. Quantification of spatial transitions or spatial gradations between slope positions can increase the accuracy of terrain parameterization for geographical or ecological modeling, especially for digital soil mapping at a fine scale. Current models for characterizing the spatial gradation of slope positions based on a gridded DEM either focus solely on the parameter space or depend on too many rules defined by topographic attributes, which makes such approaches impractical. The typical locations of a slope position contain the characteristics of the slope position in both parameter space and spatial context. Thus, the spatial gradation of slope positions can be quantified by comparing terrain characteristics (spatial and parametrical) of given locations to those at typical locations. Based on this idea, this paper proposes an approach to quantifying the spatial gradation of slope positions by using typical locations as prototypes. This approach includes two parts: the first is to extract the typical locations of each slope position and treat them as the prototypes of this position; and the second is to compute the similarity between a given location and the prototypes based on both local topographic attributes and spatial context. The new approach characterizes slope position gradation in both the attribute domain (i.e., parameter space) and the spatial domain (i.e., geographic space) in an easy and practicable way. Applications show that the new approach can quantitatively describe spatial gradations among a set of slope positions. Comparison of spatial gradation of *A*-horizon sand percentages with the quantified spatial gradation of slope positions indicates that the latter reflects slope processes, confirming the effectiveness of the approach. The comparison of a soil subgroup map of the study area with the maximum similarity map derived from the approach also suggests that the quantified spatial gradation of slope position can be used to aid geographical modeling such as digital soil mapping.

1. Introduction

There is a relationship between slope positions (ridge tops, shoulder slopes, back slopes, etc.) and topographic attributes. Slope positions are geographic objects, and as such can capture geographic meanings and spatial processes. On the other hand, topographic attributes cannot fully capture these because topographic attributes contain only local information about geometric properties. A slope position, as a kind of area with a fuzzy boundary, reflects the regional terrain context as well as local geometry. Locations with the same topographic attributes might belong to different slope positions and be associated with different geomorphic processes. For example, a location on a ridge and a location in a valley might have the same slope gradient or curvature, but their geographic (spatial) context and operating geomorphic processes are completely different. Unlike topographic attributes, slope positions convey qualitative and spatial contextual information which is sometimes essential for modeling geomorphic processes.

Transitions between slope positions over space, such as from a shoulder slope to a back slope, are often gradual. Quantification of these transitions (or spatial gradations) is useful for many applications because it captures the transition of geomorphic processes over space. This is very important for example in the modeling and analysis of soil erosion at finer scale and digital soil mapping (MacMillan et al., 2000; Schmidt and Hewitt, 2004). Although there have been numerous studies of crisp classification of slope positions (e.g., Young, 1972; Conacher and Dalrymple, 1977; Speight, 1990), the spatial gradation of slope positions has not been quantified and explored until very recently.

Locations of transition between slope positions do not qualify for full membership in any of the slope position classes, and fuzzy logic is designed to express partial memberships in different classes (Zadeh, 1965; Zimmermann, 1985; Burrough, 1989; Zhu, 1997). Also, schemes which address the occurrence issue using probability, such as Bayesian

* Corresponding author. State Key Laboratory of Resources and Environmental Information System, Institute of Geographic Sciences and Natural Resources Research, CAS, Beijing 100101, China. Tel.: +86 10 64888961; fax: +86 10 64889630.
E-mail addresses: qincz@lreis.ac.cn (C.-Z. Qin), axing@lreis.ac.cn, azhu@wisc.edu (A.-X. Zhu).

0169-555X/$ – see front matter © 2009 Elsevier B.V. All rights reserved.
doi:10.1016/j.geomorph.2009.04.003

network, cannot address the similarity issue about the transition between slope positions. Therefore the quantification of spatial gradation of slope positions suggests using a fuzzy representation scheme to express the degree to which one location belongs to prescribed slope position classes. Such fuzzy representation can be achieved first by assigning memberships of a location to a set of slope position classes, and then collecting fuzzy membership values at every location to describe the spatial gradation of slope position across a landscape.

There are two types of approaches for deriving fuzzy membership values (Deng, 2007): fuzzy clustering and semantic import (SI). The fuzzy clustering approach (e.g., Irvin et al., 1997; de Bruin and Stein, 1998; Burrough et al., 2000; Arrell et al., 2007) is based on the fuzzy *k*-means algorithm (Bezdek et al., 1984). The approach works only in the attribute domain (parameter space), and does not include spatial information or context (Burrough et al., 2001). Thus, the result from these methods sometimes lacks physical meaning (Schmidt and Hewitt, 2004).

The fuzzy clustering approach cannot extract slope positions which only exist over a very small proportion of the application area, or whose definition is based on spatial context only. In contrast, the SI approach (e.g., MacMillan et al., 2000; Schmidt and Hewitt, 2004; Dragut and Blaschke, 2006) first defines the central concept of slope positions using topographic attributes and their typical ranges; then the membership functions of topographic attributes are built and used to infer the fuzzy membership in slope positions for various locations. The key point of this approach is to establish quantitative and exact classification rules for the slope positions in terms of topographic attributes. Incomplete definition of slope positions in topographic attributes can lead to incorrect inferences (Wood, 1996). Therefore, the SI approach has limited practicability because it requires extensive user knowledge of local landforms as well as a large number of topographic attributes, thresholds, and intensive operations (Burrough, 1989). Moreover, in the SI approach, the consideration of spatial information in computing fuzzy slope positions is indirect (e.g., MacMillan et al., 2000).

We believe that typical locations of slope positions can be identified with less difficulty and higher certainty, because the locations reflect the most typical conditions (combination) of terrain attributes and unique spatial context. Using a similarity-based model (Zhu, 1997), we can compute the similarity between the typical locations of a given slope position and any other locations (i.e., cells in grid digital elevation models: DEMs) based on characteristics of both attribute and spatial domains. Shi et al. (2005) initially implemented this idea to derive fuzzy representation of some special terrain features such as broad and narrow ridges. This paper first extends this idea by proposing a prototype-based approach to quantify the spatial graduation of slope positions, and then illustrates the approach using two case studies.

2. Regional settings

2.1. Study area in Wisconsin, USA

The study area of the first application in this paper is a small watershed called Pleasant Valley in southwestern Wisconsin, USA. The elevation of the area ranges from 233 to 352 m and the average slope is 9.7°. The DEM used consists of 355 rows and 427 columns with a spatial grid resolution of 9.14 m (30 ft) (Fig. 1). The DEM was preprocessed to remove small pits, which were mostly noise created during the DEM generation process.

In this area, most ridges and valleys have been under cultivation since the late 19th century. Side-slopes are generally forested while some have been cleared for pasturing. The soil is formed from multiple layers of eolian loess of recent origin (Pleistocene era). The soils on ridges and side-slopes are relatively thin. Valleys have thick alluvial and colluvial deposits (Shi et al., 2004).

2.2. Study area in Northeastern China

In the second case study we examine how the quantification of spatial gradation of slope positions contributes to digital soil mapping. The study area is a small (about 60 km^2) low-relief part of the Nenjiang watershed in Northeastern China (Fig. 2). The relief of the area is about 100 m and the average slope gradient is 2°. The grid size of the DEM used is 10 m.

Current land use in this area is mainly corn and wheat farming. The soils are formed on silty loam loess deposits, and the parent material is almost the same in the whole area. The soil subgroup in the Chinese soil taxonomy (Gong, 2003) was chosen as the basic unit for digital soil mapping. There are six soil subgroups in the study area (Zhu et al., in press): Mollic Bori-Udic Cambosols, Typic Hapli-Udic Isohumpsols, Typic Bori-Udic Cambosols, Lithic Udi-Orthic Primosoils, Pachic Stagni-Udic Isohumpsols, and Typic Haplic-Fibric Histic Stagnic Gleyosols. The Soil Land Inference Model (SoLIM) (Zhu et al., 1996, 2001; Zhu, 1997) was employed to map the soils in the area (Fig. 3). The required knowledge of soil–environment relationships was derived using the purposive sampling approach (Zhu et al., in press). The accuracy of the soil map determined through field validation at 64 sites is roughly 72% (Zhu et al., in press).

3. Materials and methods

3.1. System of slope positions

In this paper, we adopt a two-tier hierarchical system of slope positions (Fig. 4). The first tier in this system mainly considers the spatial context along a downslope profile and consists of five slope

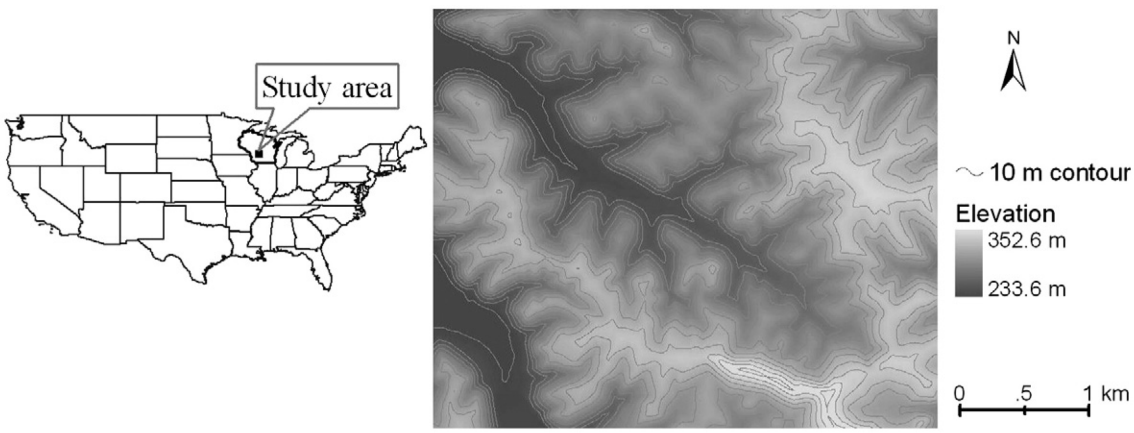

Fig. 1. Map of the Pleasant Valley study area, Wisconsin, USA.

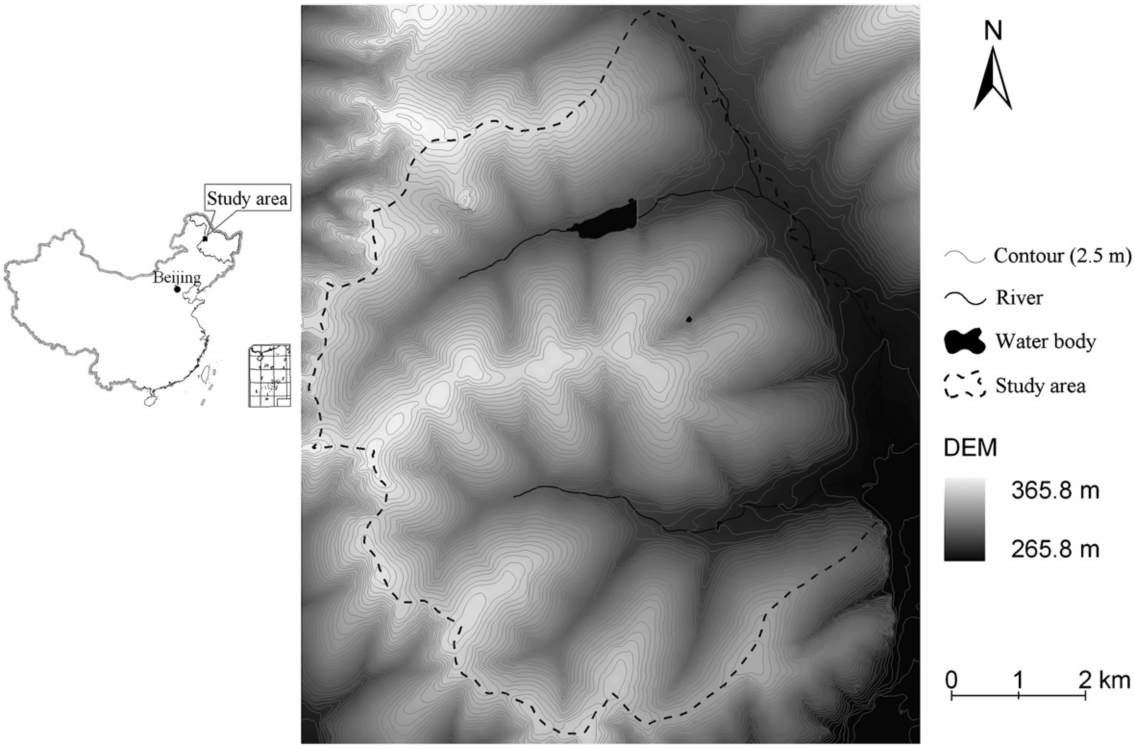

Fig. 2. Map of the Nenjiang study area, Northeastern China.

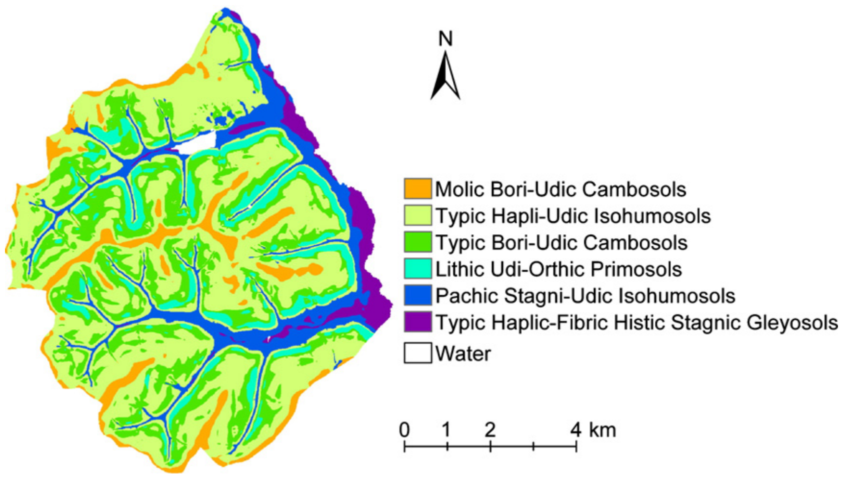

Fig. 3. Map of soil subgroups in the Nenjiang study area (after Zhu et al., in press).

First tier

Ridge (summit) (SMT)
Slope shoulder (SHD)
Backslope (BKS)
Footslope (FTS)
Valley (VLY)

Second tier

		Contour curvature		
		convex	planar	concave
Profile curvature	convex	Divergent SHD (DSHD)	Planar SHD (PSHD)	Convergent SHD (CSHD)
	planar	Divergent BKS (DBKS)	Planar BKS (PBKS)	Convergent BKS (CBKS)
	concave	Divergent FTS (DFTS)	Planar FTS (PFTS)	Convergent FTS (CFTS)

Fig. 4. System of slope positions.

positions: ridge (or summit), shoulder slope, back slope, foot slope, and valley. This taxonomy is similar to the system of landform units proposed by Ruhe (1969). These positions generally form a sequence from the top to the bottom of a slope.

The second tier in the system is a subdivision of the first tier by considering the convexity and concavity of surface shape along a contour. It is similar to the system of slope positions proposed by Pennock et al. (1987), Dikau (1989) and Schmidt and Hewitt (2004). Three of the five first-tier slope positions (shoulder slope, back slope, and foot slope) are further divided into convex (or divergent), planar, or concave (or convergent) in terms of contour curvature. Therefore, the second tier contains a total of eleven slope positions (Fig. 4): ridge, divergent shoulder slope, planar shoulder slope, convergent shoulder slope, divergent back slope, planar back slope, convergent back slope, divergent foot slope, planar foot slope, convergent foot slope, and valley.

The slope positions in the proposed system can be seen as a basic component of a landform. A combination of these slope positions can be used to describe any kinds of geomorphologic objects such as terraces and catchments.

3.2. Generation of prototypes of slope positions

According to the prototype theory, a prototype represents a category which reflects the central tendency of features or properties of real instances (Rosch, 1973; Minda and Smith, 2001). A prototype can be either a real example of a category or a specific definition. For example, the prototype of the category "furniture" can be instantiated with a chair, a table, etc. The prototype "furniture" can also be descriptively defined with its components, function, difference from other things, etc. The prototype "shoulder slope" is an example in geomorphology. It can be described as locations with maximum change of slope gradient adjacent to both a ridge and a back slope. The prototype can also be assigned to real locations in a study area. A category may have more than one prototype; therefore, prototypes of the same category could be different. For example, the prototypes of the shoulder slope could be located in different sides of a hill with different values of profile curvature.

By creating a category prototype and defining membership gradations based on the difference between a new instance and the prototype, the spatial gradation of slope positions can be inferred. As Qi et al. (2006) discussed, prototypes are suited to represent spatial features with the following four characteristics: 1) internal heterogeneity, 2) indeterminate boundaries, 3) relative definition of categories, and 4) changeable criteria. By nature slope positions exist as a continuum both in spatial and attribute domains, and have internal heterogeneity (e.g., locations with different topographic attribute values in a back slope) and indeterminate boundaries. The definition of slope positions is always relative, and both the prototype of a slope position and the criteria for determining membership in a slope position class may change depending on the amount of regional knowledge. Consequently, the prototype-based approach can be a potential solution to fuzzy quantification of slope positions and their spatial gradation.

The prototype-based approach consists of two parts. The first part is to generate prototypes of a slope position that define the central concept of the position. The second part is to determine membership gradation and derive the similarity of every cell to prototypes of each slope position.

In this study, we take typical locations of a slope position as its prototype, because the typical locations reflect the most typical conditions (combination) of terrain attributes and the unique spatial context under which the given slope position appears. The typical locations can be identified without difficulty, so the model and approach represented in the latter part of this paper are easily realizable.

The prototypes of slope positions can be found in two ways (Shi et al., 2005). One is definition-based, using typical location identification algorithms or a set of simple rules based on both geomorphologic definitions and topographic attributes. The other is knowledge-based, in which local experts manually delineate the typical locations. Methods for identifying typical terrain positions such as ridge lines and valleys have been developed for many applications (e.g., Peucker and Douglas, 1975; O'Callaghan and Mark, 1984). The generation of prototypes does not affect the method of calculating the membership (similarity) between the prototypes and other locations. The prototypes extracted should be as representative as possible and yet not so numerous as to make the calculation of membership too time-consuming. Therefore, some rules based on terrain attributes and domain knowledge could be further applied to filtrate the prototypes extracted. For example, an automatic algorithm of drainage network extraction could be used to prepare candidates for the prototypes of valley. Then the prototypes could be obtained by filtrating these candidates by a rule that the slope gradient of a valley should be less than 1°. Interested readers are referred to Shi et al. (2005) for a detailed description of the process and procedures for selecting prototypes.

3.3. Quantification of similarity to prototypes

The typical locations of a slope position, used as prototypes, have the highest membership value in the slope position class among all locations under consideration (i.e., 1 if the range of membership is the interval [0, 1]). The membership value in each slope position class can be derived for any cell based on its similarity to the prototypes. The similarity is measured in both terrain attribute and spatial domains.

There are three steps to calculate the similarity of a cell (i, j) (location P_{ij}) to a given slope position (C) based on terrain attributes (Fig. 5). Here m represents the number of prototypes for C and n represents the number of terrain attributes.

3.3.1. Step 1

In this step, a fuzzy membership function is used to evaluate the similarity between location P_{ij} and a prototype based on a single terrain attribute (Shi et al., 2005):

$$\begin{cases} S_{ij}^{v,t} = \exp\left\{\left(\left|A_{ij}^{v} - A^{v,t}\right| \Big/ w_1\right)^2 \ln(k_1)\right\} & , \quad A_{ij}^{v} < A^{v,t} \\ S_{ij}^{v,t} = 1 & , \quad A_{ij}^{v} = A^{v,t} \\ S_{ij}^{v,t} = \exp\left\{\left[\left(A_{ij}^{v} - A^{v,t}\right) \Big/ w_2\right]^2 \ln(k_2)\right\} & , \quad A_{ij}^{v} > A^{v,t} \end{cases} \quad (1)$$

where $S_{ij}^{v,t}$ is the similarity between the cell P_{ij} and a prototype t ($t \in [1\ldots m]$) based on the v-th terrain attribute ($v \in [1\ldots n]$) whose value at point

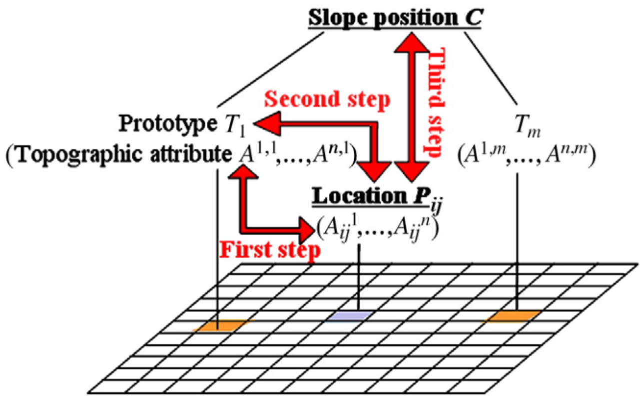

Fig. 5. Framework of the approach to the quantification of the spatial gradation of slope positions.

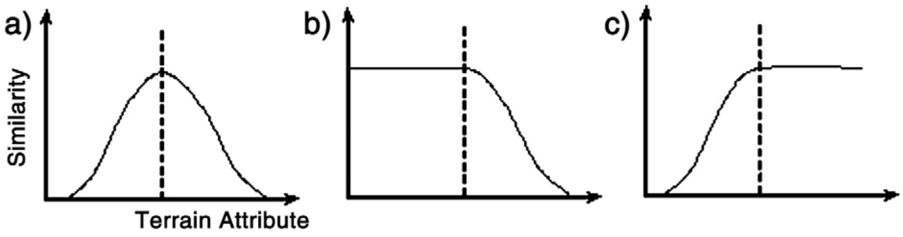

Fig. 6. Three types of similarity curves: a) *bell-shaped* function; b) *z-shaped* function; c) *s-shaped* function.

P_{ij} is A^v_{ij} and $A^{v,t}$ is the value of the v-th terrain attribute for the prototype t. The two sets of w and k are shape-controlling parameters which can be used to adjust the shape of the membership function. When $w_1 = w_2$ and $k_1 = k_2 \neq 1$, this model produces a so-called *bell-shaped* symmetric curve (Fig. 6a). When $k_1 = 1$ and $k_2 \neq 1$, this model approaches a *z-shaped* function (Fig. 6b), and when $k_1 \neq 1$ and $k_2 = 1$, it approaches an *s-shaped* function (Fig. 6c). k_1 is often set to 0.5 when an *s-* or *bell-shaped* function is used. This means that the membership value decreases to 0.5 when the terrain attribute value is less than the corresponding value for the prototype by the value of w_1. k_2 is also often set to 0.5 when a *z-* or *bell-shaped* function is used, which means that the membership value decreases to 0.5 when the terrain attribute value exceeds the corresponding value for the prototype by the value of w_2.

A real application using a membership function depends on domain and regional knowledge about the slope positions in the study area. For example, the shape of a typical back slope is considered to be steep and nearly straight along a profile. So an *s-shaped* function for slope gradient can be used to compute the similarity between a location and the prototype of back slopes based on gradient. In contrast, a *bell-shaped* function for profile curvature will be used to compute the similarity between a location and the prototype of back slopes based on curvature.

3.3.2. Step 2

This step integrates the individual similarities based on individual terrain attributes to obtain an overall similarity between P_{ij} and the prototype t. In this paper, a minimum operator based on the limiting-factor principle in ecology is used to compute the similarity (Zhu and Band, 1994):

$$S^t_{ij} = \left(\min S^{1,t}_{ij}, S^{2,t}_{ij}, \ldots, S^{v,t}_{ij}, \ldots, S^{n,t}_{ij}\right) \tag{2}$$

where S^t_{ij} is the overall similarity of P_{ij} to prototype t; and n is the number of terrain attributes.

3.3.3. Step 3

This step computes the similarity of P_{ij} to slope position C. For each slope position, each of the m prototypes has different importance in deriving fuzzy membership for P_{ij}. For example, the prototypes of back slope could be with different values of slope gradient for different sides of a hill in the study area. During the computation of fuzzy membership for a location in a north-facing slope, a prototype of north-facing slopes should play a more important role than a prototype of south-facing slopes. It is reasonable to assume that the importance of a prototype to the computation of fuzzy membership for P_{ij} decreases as the distance from the prototype to P_{ij} increases. Therefore we used an inverse distance weighted function to calculate the membership value of P_{ij} in C:

$$S_{ij} = \sum_{t=1}^{m} \left(d^t_{ij}\right)^{-r} S^t_{ij} \bigg/ \sum_{t=1}^{m} \left(d^t_{ij}\right)^{-r} \tag{3}$$

where S_{ij} is the fuzzy membership of P_{ij} in C based on terrain attributes; d^t_{ij} is the Euclidean distance between P_{ij} and prototype t; and r is the distance decay factor. Based on trials, r is set to 8.

These three steps were repeated for each slope position at every cell in the gridded DEM to derive the similarity map of each slope position across the study area. Collection of these membership maps represents the spatial gradation of slope positions over the area, as discussed earlier. For every cell, there is an array of membership values with each value representing the similarity of this cell to a slope position class.

4. Results and discussion

4.1. Wisconsin case study

4.1.1. Characterization of spatial gradation of slope positions

In this application, we quantified the spatial gradation of first-tier slope positions as defined in Section 3.1. These slope positions consist of five components: ridge, shoulder slope, back slope, foot slope, and valley.

The identification of typical locations, extraction by either rules or expert identification, is independent of the computation of the similarity between other locations and prototypes. In this study, we used topographic attributes and a set of rules to identify the typical locations. The definitions of slope positions by Pennock et al. (1987), MacMillan et al. (2000), and Schmidt and Hewitt (2004) as well as Skidmore (1990)'s relative position index (*RPI*) were combined to

Table 1
Parameter values for selecting the prototypes of slope positions in the Pleasant Valley study area.

	Ridge	Shoulder slope	Back slope	Foot slope	Valley
RPI	≥0.99	[0.9, 0.95]	[0.5, 0.6]	[0.15,0.2]	≤0.1
Profile curvature ($\times 10^{-3}$ m^{-1})	≥0	≥5	[−0.1, 0.1]	≤−5	[−0.1, 0.1]
Slope (°)	≤1		≥10		≤1
Elevation (m)	≥285				

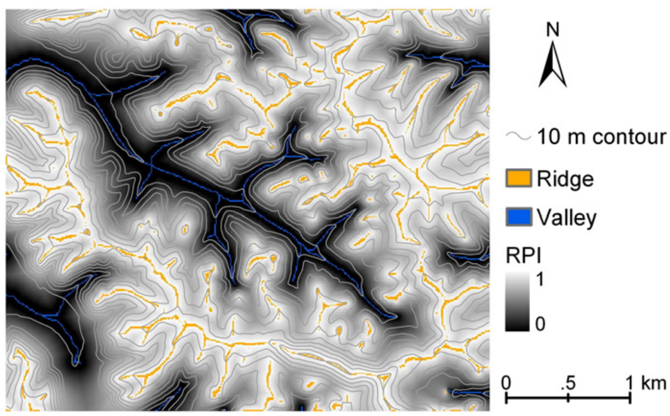

Fig. 7. Relative Position Index (*RPI*) of the Pleasant Valley study area.

Table 2
Parameter values for the membership function in the Pleasant Valley study area.

	Ridge	Shoulder slope	Back slope	Foot slope	Valley
RPI	'S'; $w_1=0.1$	'Bell'; $w_1=w_2=0.05$	'Bell'; $w_1=w_2=0.3$	'Bell'; $w_1=w_2=0.05$	'Z'; $w_2=0.1$
Profile curvature ($\times 10^{-3}$ m^{-1})	'S'; $w_1=5$	'S'; $w_1=5$	'Bell'; $w_1=w_2=5$	'Z'; $w_2=5$	'Bell'; $w_1=w_2=5$
Slope (°)	'Z'; $w_2=5$	'Bell'; $w_1=w_2=5$	'S'; $w_1=5$	'Bell'; $w_1=w_2=5$	'Z'; $w_2=5$
Elevation (m)	'S'; $w_1=5$				

'Bell': *bell-shaped* function in Fig. 3; 'Z': *z-shaped* function; 'S': *s-shaped* function.

extract the prototypes of slope positions (Table 1). The local topographic attributes used in this study include elevation, slope, and profile curvature. For profile curvature, negative value represents concave and positive value represents convex. Skidmore (1990)'s *RPI*, as a regional terrain index, gives an approximate estimate of how far a location is from a ridge or a valley. The *RPI* value of a location is calculated using the Euclidean distance to the nearest ridge divided by the sum of Euclidean distances to the nearest streamline and ridge.

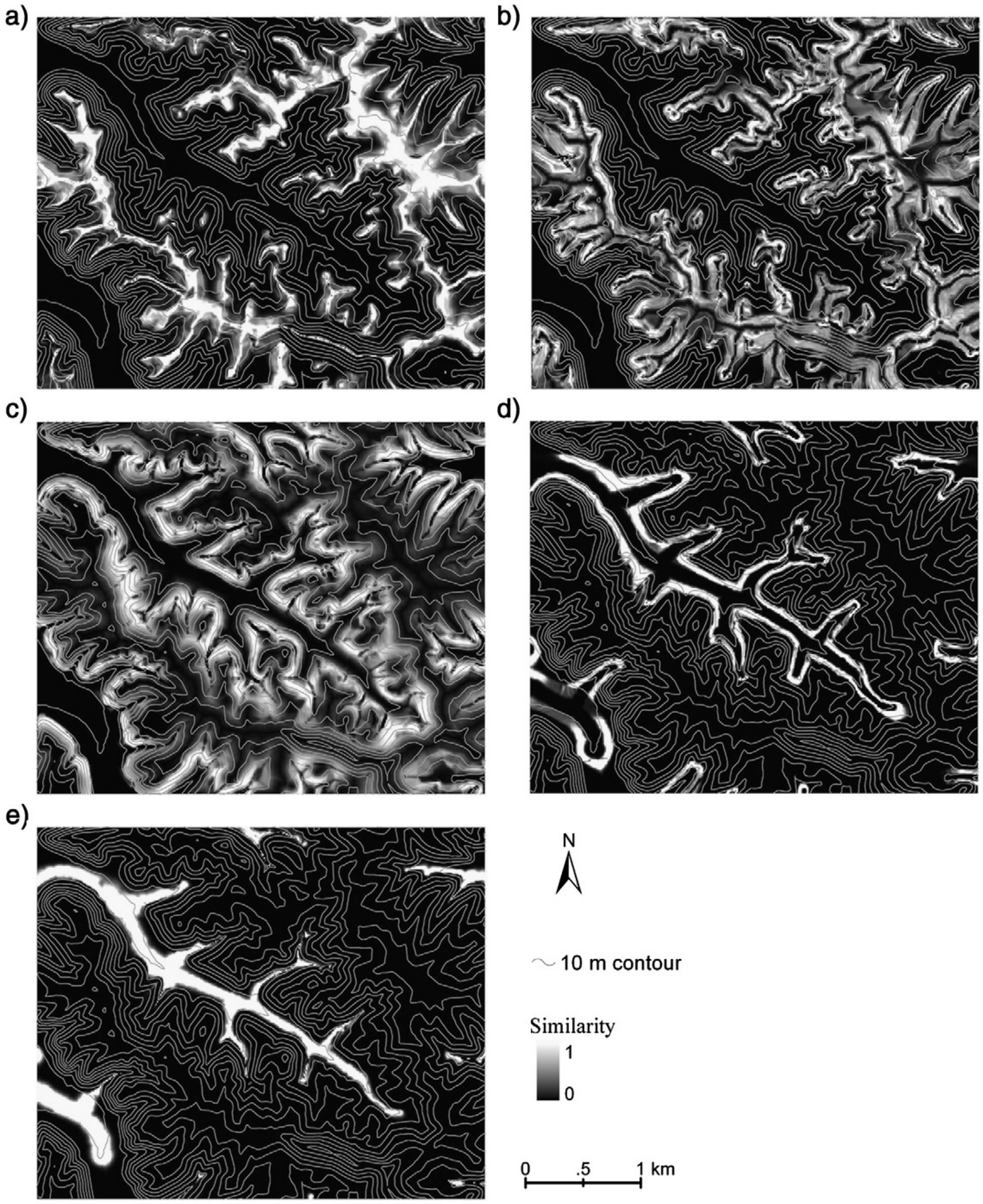

Fig. 8. Similarity maps of the Pleasant Valley study area: a) ridge; b) shoulder slope; c) back slope; d) foot slope; e) valley.

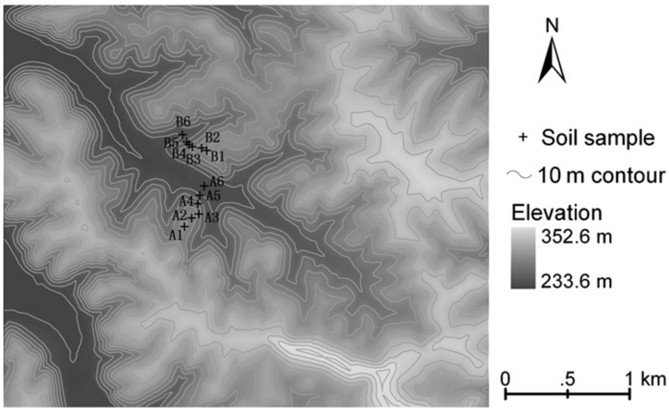

Fig. 9. Positions of 12 soil samples along the two transects in Pleasant Valley study area.

The value range of RPI is [0, 1]; 1 for a ridge and 0 for a valley. Ridges and valleys need to be defined before calculating *RPI*. In this study, the algorithm by Peucker and Douglas (1975) was applied to extract ridges (shown in yellow in Fig. 7), and that by O'Callaghan and Mark (1984) was used to extract valleys (blue in Fig. 7). The threshold of upslope contributing area for O'Callaghan and Mark (1984)'s algorithm was 0.2 km^2. Although ridges and valleys for computing *RPI* can also be used directly as the prototypes for ridges and valleys, we used the rules in Table 1 instead, to be consistent with the generation of prototypes for other slope position classes.

To characterize the spatial gradation of each slope position, the values of parameters w_1 and w_2, defining the membership function, were set by referring to the criteria for selecting the prototypes of the slope position (Table 2).

4.1.2. Results and discussion based on soil samples

The similarity maps of each slope position in the study area (Fig. 8a–e) show the spatial patterns of gradation. From the top to the bottom of the slope, the maximum similarity shows a realistic spatial sequence of slope positions, i.e., ridge (a) → shoulder slope (b) → back slope (c) → foot slope (d) → valley (e).

To examine the validity of the quantified spatial gradation, we evaluated the results in relation to soil property variation. We collected 12 soil samples along two transects (six samples on each transect; Fig. 9). The sand percentages in the *A*-horizon at these sites were determined in the laboratory. These percentages are shown in Fig. 10 along with the fuzzy membership values of five slope positions at the sample locations. Both Fig. 10a (transect A) and b (transect B) show a similar pattern of relationship between change of sand percentage and change of similarity in slope position: the sand percentages in the *A*-horizon increase when there is spatial gradation from a ridge to shoulder and back slopes. When a shoulder slope gradually transitions to the typical location of a back slope, the sand percentages in the *A*-horizon increase correspondingly along the transects. The sand percentage in the *A*-horizon decreases when a back slope gradually transitions to a foot slope. The sand percentage gradually decreases further as a foot slope gradually transitions to a valley. The soil samples with the low sand percentages in the *A*-horizon are on ridges and in valleys. The soil samples with the highest sand percentages in the *A*-horizon of both transects are always on the back slope.

The correlation between the transition pattern of similarity in slope positions and the spatial variation of soil attributes along the transects (Fig. 10) can be explained by the effect of terrain conditions on soil-forming processes. Usually, fine materials are easily preserved on a broad ridge where the surface is relatively flat, but are more susceptible to erosion in steep areas such as shoulder and back slopes.

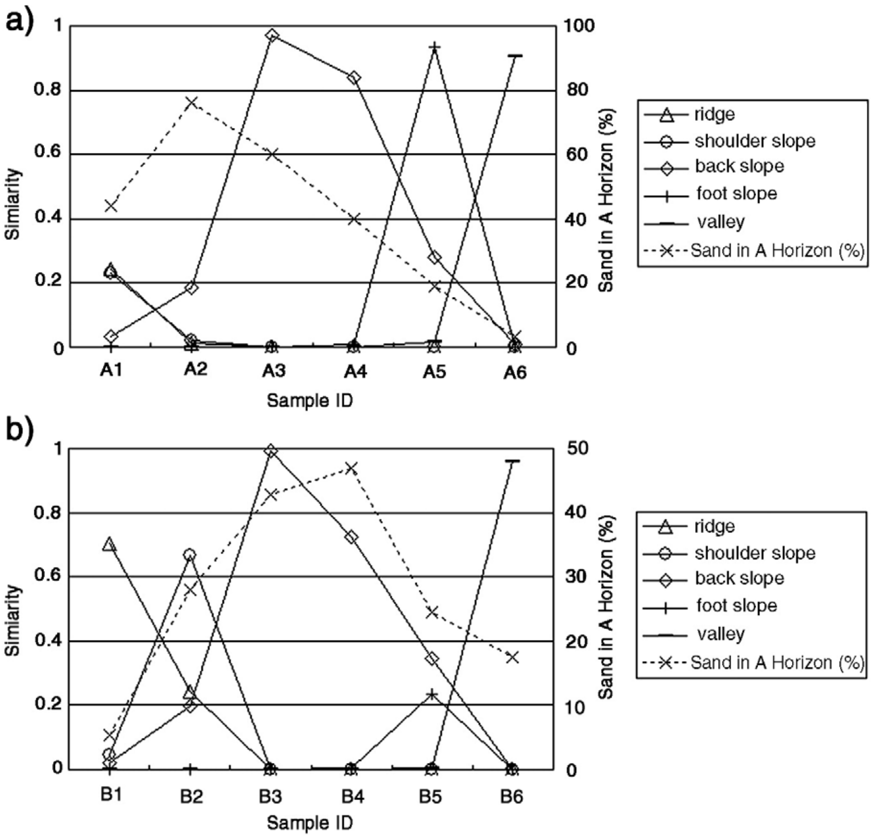

Fig. 10. Sand percentages in the *A*-horizon of two transects vs. similarity to slope positions in the Pleasant Valley study area: a) Transect A; b) Transect B.

Table 3
Parameter settings for extracting and deriving the fuzzy membership in the Nenjiang study area (abbreviations of slope positions are referred to Fig. 4).

	RPI		Profile curvature ($\times 10^{-3}$ m^{-1})		Horizontal curvature ($\times 10^{-3}$ m^{-1})		Slope gradient (°)	
	Prototype	Fuzzy inference	Prototype	Fuzzy inference	Prototype	Fuzzy inference	Prototype	Fuzzy inference
SMT	≥ 0.99	'S'; $w_1 = 0.05$	$[-0.5, 0.5]$	'Bell'; $w_1 = w_2 = 1$				
DSHD	[0.8, 0.9]	'Bell'; $w_1 = w_2 = 0.1$	≥ 0.5	'S'; $w_1 = 1$	≥ 0.5	'S'; $w_1 = 1$		
PSHD					$[-0.01, 0.01]$	'Bell'; $w_1 = w_2 = 1$		
CSHD					≤ -0.5	'Z'; $w_2 = 1$		
DBKS	[0.4, 0.6]	'Bell'; $w_1 = w_2 = 0.2$	$[-0.5, 0.5]$	'Bell'; $w_1 = w_2 = 1$	≥ 0.5	'S'; $w_1 = 1$		
PBKS			$[-0.01, 0.01]$		$[-0.01, 0.01]$	'Bell'; $w_1 = w_2 = 1$		
CBKS			$[-0.5, 0.5]$		≤ -0.5	'Z'; $w_2 = 1$		
DFTS	[0.1, 0.2]	'Bell'; $w_1 = w_2 = 0.1$	≤ -0.5	'Z'; $w_2 = 1$	≥ 0.5	'S'; $w_1 = 1$		
PFTS					$[-0.01, 0.01]$	'Bell'; $w_1 = w_2 = 1$		
CFTS					≤ -0.5	'Z'; $w_2 = 1$		
VLY	≤ 0.01	'Z'; $w_2 = 0.1$	$[-0.5, 0.5]$	'Bell'; $w_1 = w_2 = 1$			≤ 0.5	'Z'; $w_2 = 2$

In foot slope and valley areas, erosion of fine materials decreases and their deposition increases. Thus, when the slope position changes from ridge to shoulder and back slopes, the sand percentages of *A*-horizon are expected to increase. However, when the slope position changes finally into the foot slope and valley, the sand percentages of *A*-horizon are expected to decrease.

4.2. Northeastern China case study

For this second case study we used the proposed approach to derive the fuzzy representation of all 11 slope positions in the second tier of our slope position taxonomy described in Section 3.1. We also examined the potential role of quantification of spatial gradation of slope positions in digital soil mapping.

4.2.1. Deriving fuzzy representation of slope positions

The procedure for selecting prototypes and deriving the fuzzy quantification of the spatial gradation of slope positions was similar to that used in the Wisconsin case study. Table 3 lists the parameters used for this case study. We used four terrain attributes: slope, profile curvature, horizontal curvature, and *RPI*. Unlike in the Wisconsin case, elevation was not selected as one of the terrain attributes, because the relief of the study area is so gentle that elevation has little impact on soil formation and the identification of slope positions. We used horizontal curvature instead of the often-used contour (planform) curvature because the former can avoid unrealistic extremes which often occur in the latter (Shary et al., 2002). For both profile and horizontal curvatures, negative values represent concave and positive values represent convex. Some parameter values of terrain attributes used for deriving fuzzy quantification were adjusted to reflect the low-relief landscape (Table 3).

4.2.2. Results and discussion based on soil map

The membership values for the 11 slope positions were transformed based on the "hardening" operation to produce a map showing the distribution of the slope positions (hereafter referred to as the hardened map) (Fig. 11a). The hardening is done by assigning a cell to the slope position to which the similarity at that cell is the maximum. In addition to determining the slope position for each cell, the hardening process also records the membership in the slope position to which the local cell is assigned, referred to as the maximum similarity. It quantitatively characterizes how typical the local cell is of the assigned slope position and can be used to quantify the fuzziness in the hardening process. The smaller the maximum similarity is at one cell, the more ambiguous is the hardening, and the more transitional is the cell among different types of slope positions. The map of this maximum membership value (Fig. 11b) quantitatively shows the gradation of slope positions across the landscape. For example, areas where slope positions change from one to another are often where the value of maximum similarity is low, reflecting high uncertainty in assigning slope position classes to these areas.

Based on the soil map (Fig. 3) and the hardened slope position map (Fig. 11a), we calculated the proportion of soil type distributed among

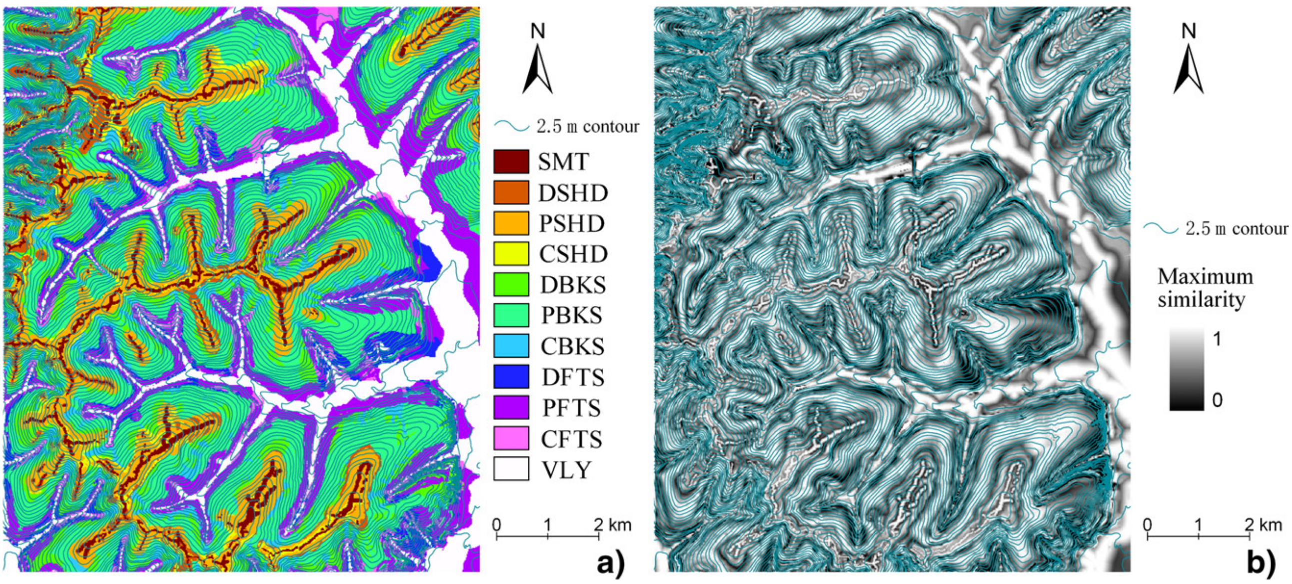

Fig. 11. Hardened map from similarity maps of slope positions in the Nenjiang study area: a) Hardened slope position map; b) Map of maximum similarity among slope positions.

slope positions with different ranges of maximum similarity (i.e., [0.8, 1] and [0, 0.5]) (Fig. 12). The range [0.8, 1] of maximum similarity refers to areas where the hardening results have the lowest ambiguity (least fuzziness). The range [0, 0.5] refers to where the hardening results have the highest ambiguity (great fuzziness).

As shown in Fig. 12a, there is an apparent relationship between the spatial distribution of slope positions and the spatial distribution of soil subgroups in areas where the hardened slope positions have little fuzziness. Mollic Bori-Udic Cambosols (i.e., soil 1 in Fig. 12) are mainly located on ridges and planar shoulder slope and planar back slopes. Typic Hapli-Udic Isohumpsols and Typic Bori-Udic Cambosols (soils 2 and 3 in Fig. 12, respectively) are mainly found on planar back slopes. Lithic Udi-Orthic Primosoils (soil 4 in Fig. 12) are distributed mainly on planar foot and planar back slopes. Pachic Stagni-Udic Isohumpsols and Typic Haplic-Fibric Histic Stagnic Gleyosols (soils 5 and 6 in Fig. 12, respectively) almost always exist in valleys. A small proportion of Pachic Stagni-Udic Isohumpsols was found on planar foot slopes. These results match the field observations of catena in the study area (Zhu et al., in press) and will be helpful to soil-landscape modeling in the area.

In areas where the hardened slope position has a high degree of fuzziness, the distribution of soil subgroups is so miscellaneous that there is no identifiable relationship between the soil distribution and the distribution of slope positions. For example, Fig. 12b shows that the Typic Hapli-Udic Isohumpsols (soil 2) are found relatively evenly in all slope positions. Actually, this soil subgroup is widely found on back slopes. Another example is Typic Haplic-Fibric Histic Stagnic Gleyosols (soil 6), which are always distributed in marshes in valleys. In Fig. 12b, Typic Haplic-Fibric Histic Stagnic Gleyosols do not occur in valleys which are areas of transition with high fuzziness on the hardened map. Therefore, if the fuzziness of slope positions is not considered, the quality of soil-landscape modeling and digital soil mapping will be degraded.

5. Conclusions

The fuzzy quantification of spatial gradation of slope positions can provide important additional terrain information to terrain-related geographical or ecological modeling, especially fine-scale digital soil mapping. This terrain information cannot be replaced by widely-used topographic attributes. Previous approaches of deriving fuzzy quantification of spatial gradation of slope positions ignore spatial information and have limited practicability.

This paper presents an approach to the quantification of spatial gradation of slope positions which first identifies typical locations of slope positions as prototypes. Then a prototype-based model is used to compute the similarity of other locations to each slope position over the landscape, based on both local topographic attributes such as elevation, slope, profile curvature, and horizontal curvature and regional terrain features such as *RPI*. The proposed approach examines the similarity in both the attribute domain (i.e., parameter space) and the spatial domain (geographic space), and thus takes into account both local topographic information and terrain context.

The approach was applied to two cases. In the Wisconsin case study, the classification of slope positions comprises five classes (ridge, shoulder slope, back slope, foot slope, and valley). This case shows that the quantified slope gradation is in good correspondence to the spatial variation of sand percentages in the *A*-horizon of soil

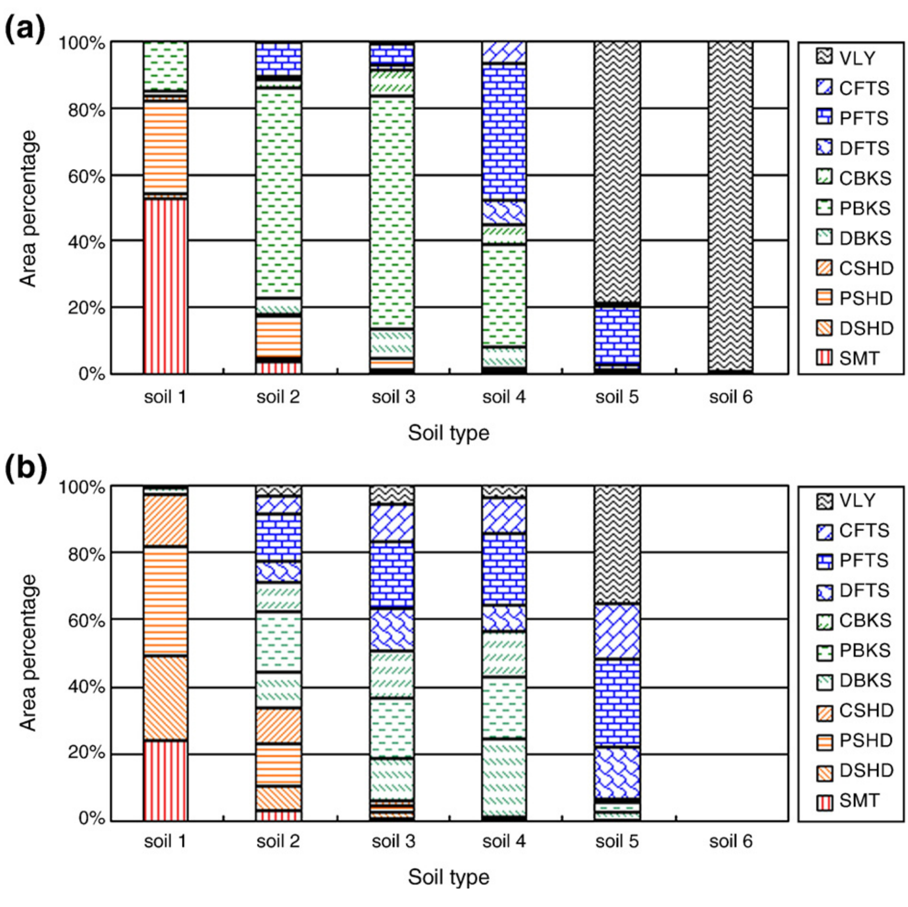

Fig. 12. Area percentage of soil subgroups distributed among slope positions with different ranges of maximum similarity in the Nenjiang study area: a) [0.8, 1]; b) [0, 0.5]. Soil 1 — Mollic Bori-Udic Cambosols; soil 2 — Typic Hapli-Udic Isohumpsols; soil 3 — Typic Bori-Udic Cambosols; soil 4 — Lithic Udi-Orthic Primosoils; soil 5 — Pachic Stagni-Udic Isohumpsols; soil 6 — Typic Haplic-Fibric Histic Stagnic Gleyosols.

samples along two transects, indicating that the approach can meaningfully quantify slope gradation.

The second application to a part of the Nenjiang watershed in Northeastern China derived the fuzzy quantification of the spatial gradation of detailed slope positions. The results were used to produce a hardened map of slope positions and a map of maximum similarity. The latter map quantitatively shows the fuzziness of a slope position assigned to each cell. The analysis combining the two maps with a soil subgroup map showed that there is a relationship between fuzzy quantification of the spatial gradation of slope positions and the spatial distribution of soil subgroups. Areas with little fuzziness (i.e., high value of maximum similarity) correspond well to a few individual soil subgroups, while areas with high ambiguity correspond to miscellaneous soil subgroups at the transitional areas of slope positions. Therefore, the fuzzy quantification of the spatial gradation of slope positions has potential in soil-landscape modeling.

The approach proposed in this paper also has implications for other geographical analyses. Slope positions are basic landform units which compose different kinds of specific geomorphic features from individual small hills to large plains and mountains (Blaszczynski, 1997). The fuzzy quantification of the spatial gradation of slope positions can provide more information for identifying and discriminating specific geomorphic features than can be provided by crisp classification of slope positions. Furthermore, the configuration of the spatial transition of slope positions influences surface water flow, transport of sediment and pollutants, and distribution of habitats for plant and animal species. Therefore, our approach is useful for a variety of resource and environmental studies.

Acknowledgements

This study was funded by the National Natural Science Foundation of China (Project Number: 40501056; 40601078), the International Partnership Project 'Human Activities and Ecosystem Changes' (Project Number: CXTD-Z2005-1) of the Chinese Academy of Sciences, National Basic Research Program of China (2007CB407207), and the Knowledge Innovation Program of the Chinese Academy of Sciences (Project Number: KZCX2-YW-Q10-1-5). Supports from the Institute of Geographical Sciences and Natural Resources Research, the State Key Laboratory of Resources and Environmental Information Systems, and the University of Wisconsin-Madison are also appreciated. The authors thank Prof. Jonathan Phillips and an anonymous reviewer for their generous efforts and constructive comments on an earlier version of this paper. We appreciate the inputs from Robert MacMillan during early conception of this paper.

References

Arrell, K.E., Fisher, P.F., Tate, N.J., Bastin, L., 2007. A fuzzy *c*-means classification of elevation derivatives to extract the morphometric classification of landforms in Snowdonia, Wales. Computers & Geosciences 33, 1366–1381.

Bezdek, J., Ehrlich, R., Full, W., 1984. FCM: the fuzzy *c*-means clustering algorithm. Computers & Geosciences 10, 191–203.

Blaszczynski, J.S., 1997. Landform characterization with Geographic Information Systems. Photogrammetric Engineering and Remote Sensing 63 (2), 183–191.

de Bruin, S., Stein, A., 1998. Soil-landscape modeling using fuzzy *c*-means clustering of attribute data derived from a Digital Elevation Model (DEM). Geoderma 83, 17–33.

Burrough, P., 1989. Fuzzy mathematical methods for soil survey and land evaluation. Journal of Soil Science 40, 477–492.

Burrough, P., van Gaans, P., MacMillan, R., 2000. High-resolution landform classification using fuzzy *k*-means. Fuzzy Sets and Systems 113, 37–52.

Burrough, P., Wilson, J., van Gaans, P., Hansen, A., 2001. Fuzzy *k*-means classification of topo-climatic data as an aid to forest mapping in the Great Yellowstone Area, USA. Landscape Ecology 16, 523–546.

Conacher, A.J., Dalrymple, J.B., 1977. The nine unit landsurface model: an approach to pedogeomorphic research. Geoderma 18, 1–154.

Deng, Y., 2007. New trends in digital terrain analysis: landform definition, representation, and classification. Progress in Physical Geography 31, 405–419.

Dikau, R., 1989. The application of a digital relief model to landform analysis. In: Raper, J.F. (Ed.), Three dimensional applications in Geographical Information Systems. Taylor and Francis, London, pp. 51–77.

Dragut, L., Blaschke, T., 2006. Automated classification of landform elements using object-based image analysis. Geomorphology 81, 330–344.

Gong, Z., 2003. Chinese Soil Taxonomy. Science Press, Beijing. pp. 203.

Irvin, B., Ventura, S., Slater, B., 1997. Fuzzy and isodata classification of landform elements from digital terrain data in Pleasant Valley, Wisconsin. Geoderma 77, 137–154.

MacMillan, R., Pettapiece, W., Nolan, S., Goddard, T., 2000. A generic procedure for automatically segmenting landforms into landform elements using DEMs, heuristic rules and fuzzy logic. Fuzzy Sets and Systems 113, 81–109.

Minda, J., Smith, J., 2001. Prototypes in category learning: the effects of category size, category structure, and stimulus complexity. Journal of Experimental Psychology: Learning, Memory, and Cognition 27, 775–799.

O'Callaghan, J., Mark, D., 1984. The extraction of drainage networks from digital elevation data. Computer Vision, Graphics, and Image Processing 28, 323–344.

Pennock, D., Zebarth, B., de Jone, E., 1987. Landform classification and soil distribution in hummocky terrain, Saskatchewan, Canada. Geoderma 40, 297–315.

Peucker, T., Douglas, D., 1975. Detection of surface specific points by local parallel processing of discrete terrain elevation data. Computer Graphics and Image Processing 4, 375–387.

Qi, F., Zhu, A.-X., Harrower, M., Burt, J.E., 2006. Fuzzy soil mapping based on prototype category theory. Geoderma 136, 774–787.

Rosch, E.H., 1973. Natural categories. Cognitive Psychology 4, 328–350.

Ruhe, R., 1969. Quaternary Landscapes in Iowa. Iowa University Press, Ames, Iowa. pp. 255.

Schmidt, J., Hewitt, A., 2004. Fuzzy land element classification from DTMs based on geometry and terrain position. Geoderma 121, 243–256.

Shary, P., Sharaya, L., Mitusov, A., 2002. Fundamental quantitative methods of land surface analysis. Geoderma 107, 1–32.

Shi, X., Zhu, A.-X., Burt, J., Qi, F., Simonson, D., 2004. A case-based reasoning approach to fuzzy soil mapping. Soil Science Society of America Journal 68, 885–894.

Shi, X., Zhu, A.-X., Wang, R.-X., 2005. Fuzzy representation of special terrain features using a similarity-based approach. In: Cobb, M., Petry, F., Robinson, V. (Eds.), Fuzzy Modeling with Spatial Information for Geographic Problems. Springer-Verlag, New York, pp. 233–251.

Skidmore, A., 1990. Terrain position as mapped from a gridded digital elevation model. International Journal of Geographical Information Systems 4, 33–49.

Speight, J.G., 1990. Landform, In: McDonald, R.C., Isbell, R.F., Speight, J.G., Walker, J., Hopkins, M.S. (Eds.), Australian Soil and Land Survey Field Handbook, (2nd edition). Inkata Press, Melbourne, pp. 9–57.

Wood, J., 1996. The geomorphological characterisation of Digital Elevation Models. Ph.D. Thesis, University of Leicester.

Young, A., 1972. Slopes. Oliver & Boyd, Edinburgh. pp. 288.

Zadeh, L.A., 1965. Fuzzy sets. Information and Control 8, 338–353.

Zhu, A.-X., 1997. A similarity model for representing soil spatial information. Geoderma 77, 217–242.

Zhu, A.-X., Band, L., 1994. A knowledge-based approach to data integration for soil mapping. Canadian Journal of Remote Sensing 20, 408–418.

Zhu, A.-X., Band, L.E., Dutton, B., Nimlos, T., 1996. Automated soil inference under fuzzy logic. Ecological Modeling 90, 123–145.

Zhu, A.-X., Hudson, B., Burt, J.E., Lubich, K., 2001. Soil mapping using GIS, expert knowledge and fuzzy logic. Soil Science Society of America Journal 65, 1463–1472.

Zhu, A.-X., Yang, L., Li, B.-L., Qin, C.-Z., Pei, T., Liu, B.-Y., in press. Construction of quantitative relationships between soil and environment using fuzzy *c*-means clustering. Geoderma.

Zimmermann, H.J., 1985. Fuzzy Set Theory and its Applications. Kluwer-Nijhoff, Boston. pp. 363.